UC San Diego
International Symposium on Stratified Flows

Title
Pulsating stratified turbulence in the upper equatorial oceans

Permalink
https://escholarship.org/uc/item/7376t5b1

Journal
International Symposium on Stratified Flows, 1(1)

Authors
Smyth, Bill
Pham, Hieu
Moum, Jim
et al.

Publication Date
2016-09-01

eScholarship.org Powered by the California Digital Library
University of California

Pulsating stratified turbulence in the upper equatorial oceans

W. Smyth[1], H. Pham[2], J. Moum[1], S. Sarkar[2],
Presenting Author W. Smyth[3]

[1]College of Earth, Ocean and Atmospheric Sciences
Oregon State University, Corvallis, Oregon
[2] Department of Mechanical and Aerospace Engineering, University of California, San Diego
[3]smythw@oregonstate.edu

Abstract

We propose a simple model for pulsating turbulence in a marginally-unstable stratified shear flow. The result compares favorably with fluctuating "deep cycle" turbulence observed in the upper equatorial Pacific ocean.

1 Introduction: the deep cycle of equatorial turbulence

Upper ocean turbulence increases dramatically within about a degree of the equator. This turbulence has important practical implications for climate because the equator is the primary site for heat uptake by the oceans. This heat may be transferred quickly to the atmosphere or retained in the ocean for many years depending on the turbulence. Our objective here is to better understand the processes that drive that turbulence.

In addition to their climatological significance, the upper equatorial oceans provide a unique natural laboratory for the study of stratified, parallel shear flows. Because the Coriolis acceleration changes sign at the equator, trade winds blow steadily to the west, driving a westward surface current (the south equatorial current, or SEC; figure 1a). This sets up a return flow at depth, the equatorial undercurrent (EUC). The westward SEC spreads away from the equator and and is therefore relatively weak, while the the eastward EUC converges on the equator and is much stronger. Solar insolation warms the upper few meters while upwelling (due to the diverging surface current and the converging undercurrent) brings cold water from below, setting up a strong vertical thermal gradient: the seasonal thermocline. The EUC is generally centered in this thermocline (figure 1b). Turbulent viscosity acts as a partial brake on the system, preventing runaway acceleration and leading instead to fluctuations about a forced-dissipative equilibrium state.

The classical picture of upper ocean structure is the so-called slab model. Turbulence, driven by wind and surface cooling, is strong in a layer that extends from the surface to a few tens of meters depth. Within that layer, water properties (e.g. density, velocity) are uniform, hence the name *surface mixed layer* (SML). Below the SML is the thermocline, where turbulence is much weaker and water properties vary with depth. While highly simplified, this picture applies in much of the world ocean. Here, well see how it changes at the equator.

Figure 1c shows the turbulent kinetic energy dissipation rate ϵ measured as a function of depth and time over seven days in fall 2008. The SML (solid curve) deepened every night, typically to 20m, as turbulence was amplified by surface cooling. The first thing to notice is that *turbulence extends far below the base of the SML*, in dramatic contrast to the slab model. Second, note that this deep turbulence varies diurnally. This suggests

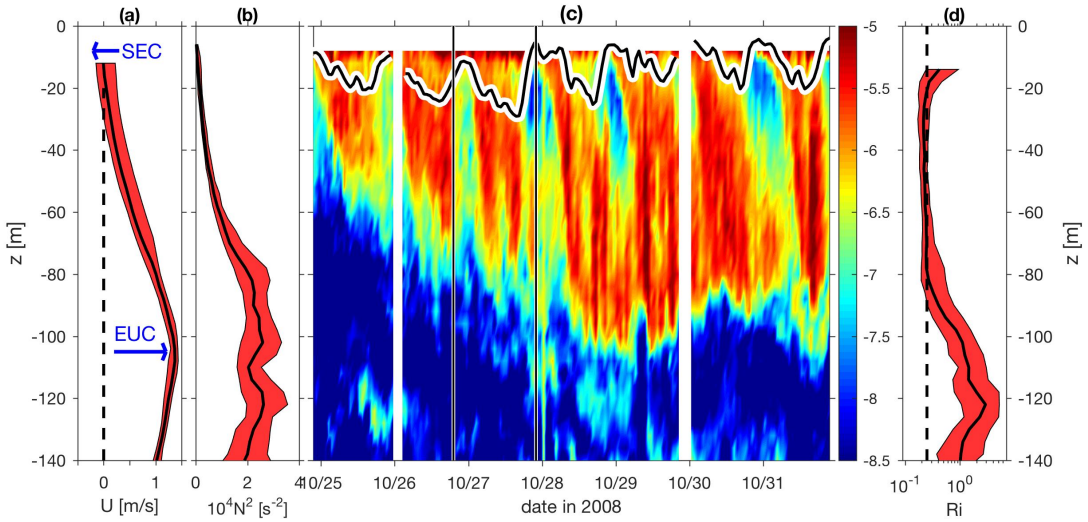

Figure 1: Profiles of the zonal velocity (a) and the squared buoyancy frequency ($N^2 = db/dz$, where b is the buoyancy) (b) measured over one week in fall 2008 (Moum et al., 2009). The solid curve is the median; the shaded area is bounded by the upper and lower quartiles. (c) Turbulent kinetic energy dissipation rate as a function of depth and time (UTC). The solid curve represents the base of the SML. Vertical lines demarcate the interval shown in figure 2. (d) Quartile range of the gradient Richardson number, $Ri = N^2/S^2$, where $S^2 = (\partial U/\partial z)^2 + (\partial V/\partial z)^2$. The dashed curve is the critical value 1/4. See Smyth et al. (2013) for further details.

that, despite the insulating effect of the SML, the deep turbulence is influenced by the diurnal surface forcing . This turbulence regime is called the deep cycle, and its mechanics have been under study since its discovery in the 1980s (Gregg et al., 1985; Moum and Caldwell, 1985).

Recent work (Smyth et al., 2013; Pham et al., 2013) has shown how the deep cycle turbulence begins each evening. The water below the SML exists in a state of *marginal instability*, in which the interaction of forcing and mixing causes the mean flow to fluctuate between stable and unstable states (Smyth and Moum, 2013). These states can be quantified using the Richardson number Ri, the ratio of squared buoyancy to squared shear. The flow is stable (unstable) if Ri is greater than (less than) a critical value, typically 1/4. In the 2008 observations, Ri fluctuated about 1/4 in a layer extending down to 80m (figure 1d). During the day, solar heating stabilizes the upper $\sim$ 10m, allowing a strong surface current to build up. At sunset, that stabilizing effect is lost. The surface current goes unstable, becomes turbulent, and mixes downward. It augments the shear of the EUC, tipping the marginally-unstable flow into a fully unstable state and thereby initiating turbulence.

While this explains the diurnal character of the deep cycle, it is not the whole story. On a given night the deep cycle can involve one or more additional pulses of turbulence. In the example shown in figure 1c, these multiple pulses are easily visible in the nights of the 26th, 27th and 28th. The origin of these pulses is not yet understood. In previous work they have been identified with internal wave interactions (Moum et al., 1992; Peters et al., 1995) and with shear instability events (Sun et al., 1998). Here, we examine the pulsations in the context of the fluctuations we expect to see in a marginally unstable regime. We advance a hypothetical mechanism for these pulsations and express it as a

pair of evolution equations for shear and turbulent kinetic energy. The model has an oscillatory solution which we compare against the observations. We propose that the mechanism exemplifies fluctuations in marginally-unstable stratified turbulence.

2 A simple model of turbulent pulses

2.1 A case study

We hypothesize that the pulses seen in deep cycle turbulence represent a quasiperiodic interaction between turbulence and shear. Consider, for example, the 26-hour period shown in figure 2. The interval begins at 10:00 local time, as solar heating approaches its noon maximum (figure 2a). For the first six hours, turbulence is weak (figure 2b), but in late afternoon a turbulent layer appears near the surface and spreads downward, extending to $\sim$ 80m depth by midnight. This turbulence reaches a maximum then decays for a few hours. But rather than decay completely it exhibits a second maximum near sunrise (t $\sim$16-22hr).

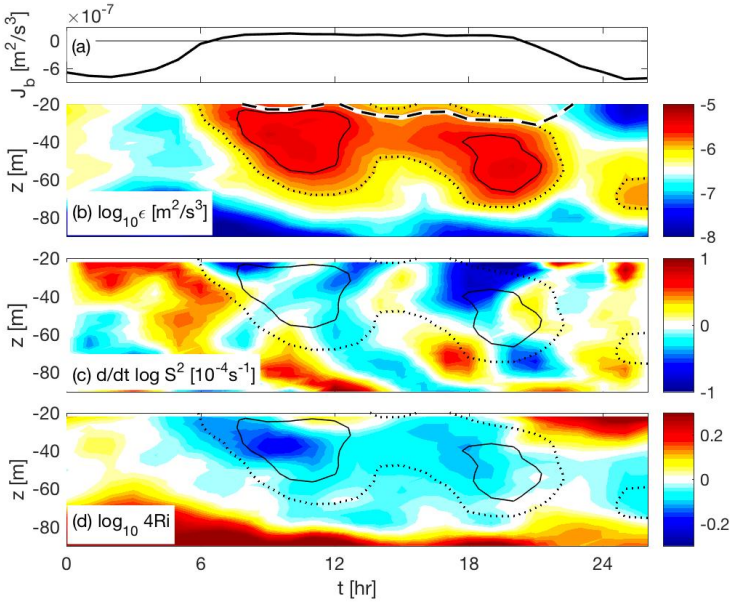

Figure 2: A case study of the deep cycle. Measurements are shown for a 26-hour period beginning at 10:00 local time, 26 October 2008 (vertical lines on figure 1c). Frames show the surface buoyancy flux J_b (a), the turbulent kinetic energy dissipation rate ϵ (b), the logarithmic time derivative of S^2 (c) and $4Ri$ (d). The dashed curve near the top of (b) shows the base of the SML.

This cycle of growing and decaying turbulence is correlated with the growth and decay of shear. The time derivative of squared shear (figure 2c) is dominated by descending bands of alternating sign. The first (the yellow-red area at the upper left) precedes the initial turbulence maximum. This corresponds to the augmentation of local shear as the daytime surface current mixes downward (Smyth et al., 2013). Subsequently, the shear oscillates, with periods of decay corresponding approximately to periods of strong turbulence. This cycle is also evident in Ri (figure 2c). During the day, Ri is generally $> 1/4$ (yellow). Each of the two turbulent events (contours on 2c) is preceded by a period in which Ri is drops to subcritical values ($< 1/4$ dark blue). In the course of each event, Ri recovers to nearly-neutral values (light blue - white).

2.2 Proposed mechanism

The example chosen for figure 2 is an especially clear one, but inspection of many other cases suggests that the chain of events is typical. On this basis, we propose a hypothetical mechanism based on the interaction of shear and turbulence in a stratified fluid forced from above.

Turbulence is forced by shear and dissipated by viscosity, while shear is forced by momentum transport from the wind and is mixed by turbulence. Just before midnight, the momentum flux from the descending daytime surface current enhances the shear, initiating the growth of turbulence. Subsequently the turbulence mixes out the shear. As the turbulence decays, though, the shear is replenished by the momentum flux from above, resulting in another episode of enhanced turbulence.

Is the proposed mechanism consistent with the observations? To answer this, we express the mechanism as a pair of evolution equations for the shear and the turbulent kinetic energy. We find that the equations have oscillatory solutions with period quite close to the observed interval between pulses. In addition, the model's mean state has turbulence dissipation rate typical of the deep cycle.

2.3 The shear equation

The SML is modeled as a slab having fixed thickness h (figure 3). A steady surface stress with friction velocity u_*^2 accelerates a uniform current u. If we take the x direction to be westward, he wind and the current correspond to the trade winds and the SEC. Underlying the SML is a shear layer of thickness H containing the deep cycle. Beneath this shear layer, the velocity is again uniform and equal to the constant U. This represents (approximately) the core of the undercurrent.

The shear in the deep cycle layer, $S = (u - U)/H$, is governed by the acceleration of the SML

$$\frac{dS}{dt} = \frac{1}{H}\frac{du}{dt} = \frac{1}{H}\frac{u_*^2 + \overline{u'w'}}{h}, \tag{1}$$

where $\overline{u'w'} < 0$ is the flux of horizontal velocity at the base of the SML and the overbar represents a horizontal average and primes denote departures from that average.

2.4 The turbulent kinetic energy equation

Within the shear layer, the specific turbulent kinetic energy $k(t) = \overline{u_i' u_i'}/2$ is assumed to be uniform in depth and to obey the usual kinetic energy equation for homogeneous turbulence:

$$\frac{dk}{dt} = -\overline{u'w'}S - \epsilon. \tag{2}$$

The first term on the right-hand side is the shear production, and ϵ is the viscous dissipation rate. The buoyancy flux term has been neglected on the grounds that it is normally small compared with ϵ.

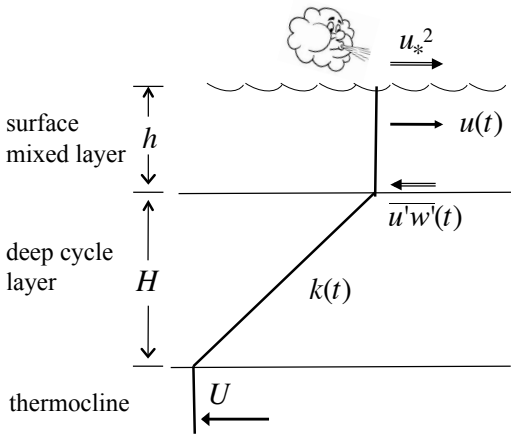

Figure 3: Schematic of the surface mixed layer with uniform velocity $u(t)$, the deep cycle layer with shear $S(t) = [u(t) - U]/H$ and turbulent kinetic energy $k(t)$ and the underlying thermocline.

2.5 Closure assumptions

We make three assumptions about the turbulence quantities ϵ and $\overline{u'w'}$ appearing in (1) and (2).

- The dissipation rate ϵ is modeled via the energy decay timescale k/ϵ. On the basis of microstructure measurements of several hundred turbulent events in the thermocline, Moum (1996) concluded that $k/\epsilon = (2.1 \pm 0.2)N^{-1}$, where N is the buoyancy frequency. Here we will use the simplified form

$$\epsilon = \frac{1}{2} N k, \tag{3}$$

  in which N is taken to be a constant.

- The velocity flux $\overline{u'w'}$ obeys

$$\overline{u'w'} = 2b_{13}k. \tag{4}$$

  The constant b_{13} is a component of the Reynolds stress anisotropy tensor and is typically negative. Values from laboratory experiments (Townsend, 1976) and direct simulations (Jacobitz et al., 1997) range between -0.21 and -0.07.

- Substitituting (3) and (4) into (2), we have

$$\frac{dk}{dt} = \left(-b_{13}S - \frac{1}{2}N \right) k. \tag{5}$$

  The turbulence is in equilibrium when

$$b_{13} = -\frac{1}{2}\frac{N}{S}. \tag{6}$$

  Consistent with observations of marginally unstable turbulence (Smyth and Moum, 2013), we assume that equilibrium is achieved when $Ri = N^2/S^2 = 1/4$, and therefore that $b_{13} = -1/8$. This value is well within the experimental range.

2.6 The model equations

With the closure assumptions listed above, we have a closed pair of evolution equations for the two unknowns $k(t)$ and $S(t)$:

$$\boxed{\frac{dk}{dt} = \left(\frac{1}{4}S - \frac{1}{2}N\right)k \; ; \qquad \frac{dS}{dt} = \frac{1}{Hh}\left(u_*^2 - \frac{1}{4}k\right).} \tag{7}$$

The system is nonlinear and does not admit a closed form solution.

2.7 The oscillatory solution

To approximate a solution of (7), we linearize about the steady solution $k = 4u_*^2$, $S = 2N$. Substituting the perturbation form

$$k = 4u_*^2 + k' \; ; \quad S = 2N + S'$$

and assuming that products of the small perturbations S' and k' are negligible, we have

$$\frac{dk'}{dt} = u_*^2 S' \; ; \quad \frac{dS'}{dt} = -\frac{1}{4Hh}k'. \tag{8}$$

These combine to give

$$\frac{d^2k'}{dt^2} = -\frac{u_*^2}{4Hh}k'. \tag{9}$$

The solution is oscillatory, with period

$$\boxed{T = \frac{4\pi\sqrt{Hh}}{u_*}.} \tag{10}$$

If the underlying assumptions are correct, this should correspond to the interval between turbulent pulses such as those in figure 2.

3 Comparison with observations

Suppose that $h = 20m$, $H = 40m$ and $u_* = 0.01ms^{-1}$. In that case (10) predicts a period of 10hr. Given the highly simplified nature of the model, this should be regarded as accurate to within a factor of two at best. Nonetheless, 10hr is very close to the interval seen in figure 2, which is 8-10hr depending how one measures.

It is also interesting to compare estimates of the viscous dissipation rate. Using the steady state expressions $k = 4u_*^2$ and $S = 2N$ in (3), we have

$$\epsilon = 2Nu_*^2 \; , \quad \text{or} \quad \epsilon = Su_*^2. \tag{11}$$

For example, assuming $u_* = 0.01ms^{-1}$ and $N = 10^{-2}s^{-1}$, we obtain $\epsilon = 2 \times 10^{-6}m^2s^{-3}$, typical of values observed in the deep cycle (figure 2a).

4 Summary and discussion

We have constructed the simplest self-consistent model that incorporates the essential processes responsible for long-period pulsations in marginally unstable stratified turbulence. With parameter choices based on previous observations and lab experiments, the model reproduces the oscillation period seen in the equatorial deep cycle (e.g. figure 2) to within a few tens of percent.

Deep cycle turbulence also involves fluctuations more rapid than those described here. For example, close examination of figure 1c shows pulsations with periods of 4 hours or less. The present model cannot account for such rapid fluctuations unless the layer thicknesses H and h are unusually small or the wind is exceptionally strong. For this and other reasons, the model begs to be generalized.

The main assumptions that underlie the present model are:

1. fluctuations in N are neglected,
2. the thickness of the DC layer is fixed,
3. shear and turbulent kinetic energy are assumed to be uniform throughout the DC layer.

In a separate article to follow, we will generalize the model to relax assumptions 1 and 2. Preliminary results indicate that the added effects are secondary, i.e. that the the physics of the long-period pulses is captured to a good approximation by the interaction of shear and turbulence.

Assumption 3, the vertical uniformity of shear and turbulence, is a critical feature without which the model would be too complicated to be useful, but it is not well-justified. In large-eddy simulations (e.g. Pham et al. (2013)) each turbulence event begins high in the DCL but generates hairpin vortices that propagate downward over a period of several hours. In a related model, (Pham et al., 2016) find that turbulence appears in layers smaller in scale than the deep cycle. The dependence on H seen in (10) suggests that disturbances of reduced vertical scale might evolve more rapidly.

We have assumed that the boundary between turbulence growth and decay is simply $Ri = 1/4$. The reality is much more complicated, with the critical Ri often being lower than 1/4 (Smyth et al., 2013; Jacobitz et al., 1997) and occasionally even higher (Thorpe et al., 2013; Li et al., 2015) depending on ambient turbulence levels. In the deep cycle, the observed median value is indistinguishable from 1/4 (e.g. figure 1d), so we retain that assumption.

This mechanism does not account for the effect of internal waves, which can alter the shear and stratification on periods of minutes to weeks and could therefore account for pulsations on shorter time scales than 9-hour interval seen in figure 2. Also not considered are rapid changes in surface forcing which could drive higher-frequency oscillations.

References

Gregg, M., Peters, H., Wesson, J., Oakey, N., and Shay, T. (1985). Intensive measurements of turbulence and shear in the equatorial undercurrent. *Nature*, 318:140–144.

Jacobitz, F., Sarkar, S., and Van Atta, C. (1997). Direct numerical simulations of the turbulence evolution in a uniformly sheared and stratified flow. *J. Fluid Mech.*, 342:231–261.

Li, L., Smyth, W., and Thorpe, S. (2015). Destabilization of a stratified shear layer by ambient turbulence. *J. Fluid Mech.*, 771:1–15.

Moum, J. (1996). Efficiency of mixing in the main thermocline. *J. Geophys. Res.*, 101(C5):12,057–12,069.

Moum, J. and Caldwell, D. (1985). Local influences on shear flow turbulence in the equatorial ocean. *Science*, 230:315–316.

Moum, J., Caldwell, D., and Paulson, C. (1989). Mixing in the equatorial surface layer and thermocline. *J. Geophys. Res.*, 94:2005–2021.

Moum, J., Hebert, D., Paulson, C., and Caldwell, D. (1992). Turbulence and internal waves at the equator. Part I: Statistics from towed thermistor chains and a microstructure profiler. *J. Phys. Oceanogr.*, 22:1330–1345.

Moum, J., Lien, R.-C., Perlin, A., Nash, J., Gregg, M., and Wiles, P. (2009). Sea surface cooling at the equator by subsurface mixing in tropical instability waves. *Nat. Geosci.*, 2:761–765.

Peters, H., Gregg, M., and Sanford, T. (1995). On the parameterization of equatorial turbulence: Effect of finescale variations below the range of the diurnal cycle. *J. Geophys. Res.*, 100:18333–18348.

Pham, H. T., Sarkar, S., Smyth, W. D., and Moum, J. N. (2016). Turbulent mixing in a marginally stable shear layer. (abstract submitted to this conference).

Pham, H. T., Sarkar, S., and Winters, K. (2013). Large-eddy simulation of deep-cycle turbulence in an upper-equatorial undercurrent model. *J. Phys. Oceanogr.*, 43(11):2490–2502.

Smyth, W. and Moum, J. (2013). Seasonal cycles of marginal instability and deep cycle turbulence in the eastern equatorial Pacific ocean. *Geophys. Res. Lett.*, 40:6181–6185.

Smyth, W., Moum, J., Li, L., and Thorpe, S. (2013). Diurnal shear instability, the descent of the surface shear layer, and the deep cycle of equatorial turbulence. *J. Phys. Oceanogr.*, 43:2432–2455.

Sun, C., Smyth, W., and Moum, J. (1998). Dynamic instability of stratified shear flow in the upper equatorial Pacific. *J. Geophys. Res.*, 103:10323–10337.

Thorpe, S., Smyth, W., and Li, L. (2013). The effect of small viscosity and diffusivity on the marginal stability of stably stratified shear flows. *J. Fluid Mech.*, 731:461–476.

Townsend, A. A. (1976). *The Structure of Turbulent Shear Flow*. Cambridge University Press, Cambridge.